

# Silver Cationization for Rapid Speciation of Sulfur-Containing Species in Crude Oils by Positive Electrospray Ionization Fourier Transform Ion Cyclotron Resonance Mass Spectrometry

Vladislav V. Lobodin,<sup>†</sup> Priyanka Juyal,<sup>†</sup> Amy M. McKenna,<sup>†</sup> Ryan P. Rodgers,<sup>\*,†,‡</sup> and Alan G. Marshall<sup>\*,†,‡</sup>

<sup>†</sup>Ion Cyclotron Resonance Program, National High Magnetic Field Laboratory, 1800 East Paul Dirac Drive, Tallahassee, Florida 32310-4005, United States

<sup>‡</sup>Department of Chemistry and Biochemistry, Florida State University, 95 Chieftain Way, Tallahassee, Florida 32306, United States

**ABSTRACT:** Silver cationization constitutes a complementary approach for analysis of petroleum components with positive-ion electrospray ionization (ESI) mass spectrometry and accesses species that lack a basic nitrogen atom and, hence, are not observed by conventional positive ESI. Four samples of different origin [Canadian bitumen, Canadian bitumen heavy vacuum gas oil (HVGO; 475–500 °C) and South American and Middle East heavy crude oils, all high in sulfur content] were used to study silver cationization by (+) ESI. Cationization with Ag<sup>+</sup> is essentially instantaneous and accesses hydrocarbons and nonpolar sulfur-containing heteroatom classes (e.g., S<sub>n</sub> and S<sub>n</sub>O<sub>m</sub>), providing an attractive alternative to time-consuming derivatization by S-methylation to ionize sulfur-containing species. For each sample, we compare Ag<sup>+</sup> cationization (+) ESI to conventional (+) ESI with formic acid to promote ion formation. Other ionization methods, such as chemical ionization (CI), field desorption (FD), matrix-assisted laser desorption ionization (MALDI) chemical ionization, field desorption ionization, and MALDI, are low in throughput and/or involve thermal processes that may degrade substrate molecules from non-volatile high-boiling petroleum components. Mix-and-spray Ag<sup>+</sup> cationization avoids tedious separation and time-consuming derivatization and results in the rapid speciation of sulfur-containing compounds in petroleum and its fractions without the need for thermal desorption.

## INTRODUCTION

At a time when the worldwide oil production trends are shifting toward production of sour, heavier crude oils, the health, safety, and environmental concerns associated with higher sulfur content oils have come to the forefront. Organic sulfur in fuels upon combustion forms toxic SO<sub>x</sub> species that are a major cause for acid rain, which, in turn, disturbs the pH balance of soil and water bodies and harms vegetation and ecosystems. They interact with other gases and particles in air to form airborne sulfates also implicated in causing respiratory diseases and aggravating heart disease and asthma. High-sulfur fuels decrease the efficacy of catalytic converters, poison NO<sub>x</sub> adsorbers, and contribute to particulate emissions. Governmental specifications and consumer demands therefore mandate a drastic cut in sulfur levels in finished fuels.<sup>1–3</sup> The petroleum industry faces a major challenge to limit organic sulfur to produce environmentally benign fuels, requiring highly active catalysts and rigorous hydroprocessing to remove sulfur and nitrogen compounds and produce cleaner transportation fuels that can meet increasingly stringent regulations.<sup>3,4</sup>

The molecular structure of different sulfur-containing compounds determines their behavior during upgrading processes.<sup>5</sup> Removal of feedstock sulfidic, disulfidic, and thiol sulfur does not present much difficulty to the refiners. However, the challenge lies in aromatic sulfur compounds, such as benzothiophenes, dibenzothiophenes, and their alkylated derivatives, which are refractory to hydrodesulfurization.<sup>6</sup> A better understanding of the structure of sulfur species in petroleum is necessary for an improved knowledge of the

mechanisms and kinetics of conversion processes to facilitate the development of better hydrodesulfurization catalysts and optimize processing conditions.<sup>7</sup> Advancements in alternative desulfurization approaches, such as biocatalysts and oxidative desulfurization, also depend upon a comprehensive structural knowledge of those compounds.<sup>8–10</sup>

Heavy crude oils and bitumen are extraordinarily chemically complex, with tens of thousands of distinct molecular elemental compositions. Fourier transform ion cyclotron resonance (FT-ICR) mass spectrometry<sup>11</sup> enables resolution and unique elemental compositional assignments, revealing heteroatom class (N<sub>n</sub>O<sub>m</sub>S<sub>s</sub>), type (DBE = number of rings plus double bonds to carbon), and carbon number.<sup>11–28</sup> Electrospray ionization mass spectrometry (ESI–MS) identifies polar compound classes by generation of protonated or deprotonated molecules ([M + H]<sup>+</sup> or [M – H]<sup>–</sup> ions).<sup>22,29–31</sup> For example, (–) ESI efficiently ionizes carboxylic acids and, thus, preferentially detects sodium and calcium naphthenates in petroleum crude oil and its deposits.<sup>32–36</sup> However, the range of molecules ionized by electrospray is limited by the acidity/basicity of the analytes and the ESI reagents. Neutral, nonpolar molecules that are not ionic in solution or not readily ionized by Brønsted or Lewis acid/base chemistry are not typically accessed by ESI.<sup>29,37,38</sup> Positive-ion ESI typically involves protonation of basic species by dilute formic or acetic acid.

Received: September 20, 2013

Revised: December 2, 2013

Published: December 13, 2013

Sulfur and hydrocarbon (HC) compound classes are not sufficiently basic.

S-Methylation reaction of sulfur compounds to form sulfonium cations can be particularly useful in highlighting nonpolar sulfur heteroatomic species for enhanced detection by ESI–MS.<sup>20,39</sup> The chemistry is based on electrophilic attack on sulfur by a strong methylating reagent with the formation of a S-methyl sulfonium salt in solution prior to ESI. Another way to improve ESI efficiency for sulfur compounds is to introduce a complexing reagent that binds to the sulfur atom to produce a positively charged ion. Roussis and Proulx examined Ag<sup>+</sup> adducts with heavy aromatic petroleum fractions and non-boiling petroleum fractions to speciate aromatic HCs by ESI–MS. They examined several ionic compounds, such as ammonium acetate, ammonium fluoride, copper acetate, etc., the best of which was AgNO<sub>3</sub>.<sup>40,41</sup> Silver complexation has previously been applied to ESI of alkenes, arenes, polystyrenes, etc. by ESI–MS.<sup>42–44</sup> The complexes can form by cation– $\pi$  interaction, host–guest, or donor–acceptor chemistry. Rudzinski et al. have reported the use of Pd<sup>II</sup> for detection of polycyclic aromatic sulfur heterocycles (PASHs) in petroleum samples.<sup>45</sup> The sulfur-containing compounds were detected as molecular ions, and the efficiency of the process depended upon many parameters, including sample/Pd<sup>II</sup> ratio, sample flow rate, solvent composition, etc.

Here, we employ silver trifluoromethanesulfonate (silver triflate, CF<sub>3</sub>SO<sub>3</sub>Ag, AgOTf) for (+) ESI FT-ICR MS for characterization of heavy crude oils, distillate, and bitumen samples by silver cationization. Silver triflate is a highly polar reagent with high solubility in nonpolar solvents used for dissolution of petroleum samples. The stability and non-nucleophilicity of the triflate anion allow it to separate from the electron-deficient silver cation, rendering it highly electrophilic and, thus, favorable for complex formation. Complex formation involves interaction of reactive silver cation (Ag<sup>+</sup>) with sources of electrons with  $\pi$  or  $\sigma$  electrons to share. The complexes may form with donor atoms (both basic and nucleophilic) and also with the  $\pi$  electron system of aromatic HCs. A compositionally complex mixture, such as crude oil, offers many reactive sites to complex with a silver cation. We compare our results to those for conventional ESI with weak organic acids and find that cationization with silver triflate results in rapid speciation of sulfur-containing compounds in petroleum and its fractions without the need for time-consuming derivatization.

## EXPERIMENTAL SECTION

**Samples and Reagents.** Canadian bitumen (C, 82.23%; H, 10.08%; N, 0.52%; and S, 5.54%), Canadian bitumen heavy vacuum gas oil (HVGO; 475–500 °C) (C, 84.68%; H, 10.20%; N, 0.23%; and S, 3.78%), a Middle East heavy crude oil (C, 80.59%; H, 11.02%; N, 0.21%; and S, 3.56%), and a South American heavy crude oil (C, 83.85%; H, 10.46%; N, 0.65%; and S, 4.67%) were used to characterize selective silver cationization. Methanol and toluene [both of high-performance liquid chromatography (HPLC) grade] and concentrated formic acid (HCOOH) were purchased from Sigma-Aldrich (St. Louis, MO). Silver triflate (AgOTf) in the highest commercially available purity was procured from Acros Organics (Geel, Belgium). Canadian bitumen and crude oils were dissolved to a final concentration of 500  $\mu$ g/mL in a 1:1 (v/v) solution of toluene/methanol, and AgOTf was added to a concentration of 50  $\mu$ g/mL. Canadian bitumen HVGO (475–500 °C) was dissolved in a 1:1 (v/v) solution of toluene/methanol to a final concentration of 100  $\mu$ g/mL, and AgOTf was added to a concentration of 50  $\mu$ g/mL. Toluene/methanol solutions containing 1% HCOOH (protonation is the only mechanism of ionization) were used for comparison to silver cationization.

**Instrumentation.** The samples were analyzed with a custom-built FT-ICR mass spectrometer equipped with a 9.4 T horizontal 220 mm bore diameter superconducting solenoid magnet operated at room temperature<sup>46</sup> and a modular ICR data station (Predator) that facilitated instrument control, data acquisition, and data analysis.<sup>47</sup> Positive ions were generated by electrospray. Sample was delivered through a fused silica micro ESI needle with a 50  $\mu$ m inner diameter by a syringe pump at a rate of 400 nL/min under typical ESI conditions (electrospray needle, +2.2 kV; tube lens, +350 V; and heated metal capillary,  $\sim$ 10 W).<sup>48</sup> The generated ions were accumulated in an external linear octopole ion trap<sup>49</sup> for 1 s and transferred by radio frequency (rf)-only octopoles<sup>50</sup> to a 10 cm diameter, 30 cm long open cylindrical Penning ion trap. Octopoles were operated at 2.0 MHz and 240 V<sub>p-p</sub> amplitude. Broadband frequency sweep (chirp) dipolar excitation (70–700 kHz at 50 Hz/ $\mu$ s sweep rate and 350 V<sub>p-p</sub> amplitude) was followed by direct mode image current detection to yield 8 Mword time-domain data sets. A total of 200 time-domain acquisitions were co-added, Hanning-apodized, and zero-filled once before fast Fourier transformation and magnitude calculation.

**Mass Calibration and Data Analysis.** The instrument was calibrated with Agilent (Palo Alto, CA) HP mix. In addition, all mass spectra were internally calibrated on the basis of the most abundant homologous ion series. Singly charged positive ions (200 <  $m/z$  < 1200) with a relative abundance greater than six standard deviations of baseline root-mean-square (rms) noise (6 $\sigma$ ) were converted to the Kendrick mass scale<sup>51</sup> for easier identification of homologous series and exported to a spreadsheet. Calculations were constrained to <sup>12</sup>C (unlimited), <sup>1</sup>H (unlimited), <sup>14</sup>N ( $\leq$ 3 atoms), <sup>16</sup>O ( $\leq$ 4 atoms), <sup>32</sup>S ( $\leq$ 4 atoms), <sup>13</sup>C ( $\leq$ atoms), <sup>34</sup>S ( $\leq$ 1 atom), and <sup>107</sup>Ag or <sup>109</sup>Ag ( $\leq$ 1 atom), with allowance for  $\pm$ 1 ppm mass error. Further aids in molecular formula elucidation are class, double bond equivalents (DBE; number of rings plus double bonds to carbon<sup>52</sup>), and carbon number, to reflect heteroatom content, degree of unsaturation, and extent of alkylation within each homologous series. For each elemental composition (C<sub>c</sub>H<sub>h</sub>N<sub>n</sub>O<sub>o</sub>S<sub>s</sub>), the heteroatom class (N<sub>n</sub>O<sub>o</sub>S<sub>s</sub>), type (DBE), and carbon number were tabulated for generation of isoabundance-contoured DBE versus carbon number images for each heteroatom class.<sup>24</sup>

## RESULTS AND DISCUSSION

As noted above, conventional positive-ion ESI in the presence of a weak acid ionizes analytes by protonation to yield [M + H]<sup>+</sup> ions and, therefore, accesses only the most basic constituents of crude oil. Mueller et al. used S-methylation chemistry to generate positive ions from thiophenes in vacuum bottom residues for direct detection by ESI–MS.<sup>39</sup> Subsequently, we compared S-methylation followed by (+) ESI mass analysis and atmospheric pressure photoionization (APPI) mass spectrometry for speciation of sulfur-containing moieties in high-boiling petroleum fractions.<sup>20</sup> We found that S-methylation chemistry efficiently detected sulfur-containing compounds of low (but not high) DBE [conventional (+) ESI], whereas APPI accessed such species throughout the DBE range without derivatization. However, S-methylation remains useful for S-speciation of distillates or lighter oils and fractions, for which DBE < 20.

**Rationale for the Choice of Silver Triflate.** Stability of a silver–analyte complex depends upon the donor molecule basicity, i.e., the ability of the ligand to share its electrons (nucleophile) with the electron-deficient silver ion. Ag<sup>+</sup> forms the strongest bonds with phosphorus and sulfur atoms, whereas the weakest bonds are formed with oxygen.<sup>31,53</sup> We therefore expect that the addition of silver triflate to petroleum samples should yield Ag<sup>+</sup> adducts observable by (+) ESI for otherwise non-detectable sulfur-containing compounds.

$^{107}\text{Ag}$  and  $^{109}\text{Ag}$ . Because silver exhibits two almost equally abundant natural isotopes (51.84%  $^{107}\text{Ag}$  and 48.16%  $^{109}\text{Ag}$ ), a silver-cationized (+) ESI mass spectrum results in a doublet for each elemental composition, corresponding to  $[\text{M} + ^{107}\text{Ag}]^+$  and  $[\text{M} + ^{109}\text{Ag}]^+$  ions. Although the mass spectrum thus contains twice as many peaks as  $[\text{M} + \text{H}]^+$  ions produced by conventional ESI, the additional peaks are readily resolved by ultrahigh-resolution FT-ICR MS. For example, Figure 1 shows

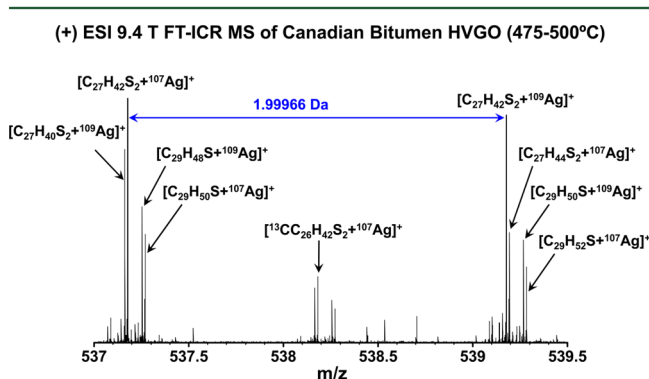


**Figure 1.** Mass scale-expanded segment (537–539.5 Da) of the (+) ESI FT-ICR mass spectrum of Canadian bitumen HVGO (475–500 °C) with AgOTf. Note the doublets corresponding to  $[\text{M} + ^{107}\text{Ag}]^+$  and  $[\text{M} + ^{109}\text{Ag}]^+$  for each silver-cationized elemental composition.

a mass scale-expanded segment from the (+) ESI FT-ICR mass spectrum from Canadian bitumen HVGO (475–500 °C) in the presence of AgOTf. Table 1 lists measured  $m/z$ , peak relative magnitude (if >5%), assigned elemental composition, and mass error [in parts per billion (ppb)] for the mass segment, 537–539.5 Da. The doublets corresponding to  $[\text{M} + ^{107}\text{Ag}]^+$  and  $[\text{M} + ^{109}\text{Ag}]^+$  ions are fully resolved for every silver-cationized elemental composition throughout the mass spectrum. Moreover, the distinctive isotope distribution because of the presence of silver isotopes enables further verification of elemental composition assignments. Thus, for example, although the possible mass difference of 0.074 mDa ( $\text{H}_5^{107}\text{Ag}$  versus  $\text{C}_4\text{S}_2$ ) that requires ultrahigh resolving power ( $m/\Delta m_{50\%} > 6\,800\,000$  at 500 Da) cannot be resolved in the broadband FT-ICR mass spectrum, detection of the corresponding  $\text{H}_5^{109}\text{Ag}$  isotopomer provides additional evidence for the correct molecular formula assignment, because the presence of the  $^{109}\text{Ag}$  isotopic peak confirms that the ( $\text{H}_5^{107}\text{Ag}$  versus  $\text{C}_4\text{S}_2$ ) peak derives from  $^{107}\text{Ag}$  and not  $\text{C}_4\text{S}_2$ .

Figure 2 shows sulfur-containing heteroatom class distributions derived from a silver cationized (+) ESI FT-ICR mass spectrum for a Canadian bitumen distillate. The  $[\text{M} + ^{107}\text{Ag}]^+$  and  $[\text{M} + ^{109}\text{Ag}]^+$  ions within a class are readily recognized from the silver isotopomer natural abundances. Elemental composition assignments are further corroborated by the identical isoabundance-contoured plots of DBE versus carbon number based on  $^{107}\text{Ag}^+$  or  $^{109}\text{Ag}^+$  cationized  $\text{S}_1$  class components.

**Access to Sulfur-Containing Components by  $\text{Ag}^+$  Cationization.** Figure 3 shows heteroatom class distributions derived from silver cationization ( $[\text{M} + \text{Ag}]^+$  ions) and conventional ( $[\text{M} + \text{H}]^+$  ions) ESI for each of four high-sulfur petroleum samples: Canadian bitumen, Canadian bitumen HVGO (475–500 °C), a Middle East heavy crude oil, and a South American heavy crude oil. Conventional (+) ESI with 1% HCCOH favors  $\text{N}_1$  and  $\text{N}_1\text{S}_1$  classes at much higher abundance

**Table 1.** Elemental Composition Assignment for Peaks (of Relative Abundance  $\geq 5\%$ ) in Mass Segment (537–539.5 Da) from the (+) ESI FT-ICR Mass Spectrum of Canadian Bitumen HVGO (475–500°C) in the Presence of AgOTf

$m/z$	relative magnitude (%)	elemental composition	mass error (ppb)
537.07081	5.0	$[\text{C}_{25}\text{H}_{32}\text{S}_3^{109}\text{Ag}]^+$	-15
537.08679	7.7	$[\text{C}_{25}\text{H}_{34}\text{S}_3^{107}\text{Ag}]^+$	-25
537.14092	7.3	$[\text{C}_{26}\text{H}_{38}\text{OS}_2^{107}\text{Ag}]^+$	-52
537.15743	5.1	$[\text{C}_{27}\text{H}_{40}\text{S}^{34}\text{S}^{107}\text{Ag}]^+$	-81
537.16133	60.0	$[\text{C}_{27}\text{H}_{40}\text{S}_2^{109}\text{Ag}]^+$	-32
537.17395	7.3	$[\text{C}_{30}\text{H}_{38}\text{S}^{107}\text{Ag}]^+$	-23
537.17731	76.7	$[\text{C}_{27}\text{H}_{42}\text{S}_2^{107}\text{Ag}]^+$	-40
537.21548	5.6	$[\text{C}_{28}\text{H}_{44}\text{OS}^{109}\text{Ag}]^+$	-50
537.23145	6.2	$[\text{C}_{28}\text{H}_{46}\text{OS}^{107}\text{Ag}]^+$	-42
537.25185	43.4	$[\text{C}_{29}\text{H}_{48}\text{S}^{109}\text{Ag}]^+$	-14
537.26784	40.0	$[\text{C}_{29}\text{H}_{50}\text{S}^{107}\text{Ag}]^+$	-24
538.16469	16.9	$[\text{C}_{26}\text{H}_{40}\text{S}_2^{109}\text{Ag}]^+$	-14
538.18067	21.0	$[\text{C}_{26}\text{H}_{42}\text{S}_2^{107}\text{Ag}]^+$	-24
538.25521	13.2	$[\text{C}_{28}\text{H}_{48}\text{S}^{109}\text{Ag}]^+$	-31
538.27119	10.6	$[\text{C}_{28}\text{H}_{50}\text{S}^{107}\text{Ag}]^+$	-42
538.44071	5.0	$[\text{C}_{39}\text{H}_{56}\text{N}]^+$	-32
538.53460	7.2	$[\text{C}_{38}\text{H}_{68}\text{N}]^+$	-52
539.08645	6.7	$[\text{C}_{25}\text{H}_{34}\text{S}_3^{109}\text{Ag}]^+$	-34
539.10244	8.1	$[\text{C}_{25}\text{H}_{36}\text{S}_3^{107}\text{Ag}]^+$	-26
539.14060	6.3	$[\text{C}_{26}\text{H}_{38}\text{OS}_2^{109}\text{Ag}]^+$	-23
539.15658	9.3	$[\text{C}_{26}\text{H}_{40}\text{OS}_2^{107}\text{Ag}]^+$	-34
539.17306	5.5	$[\text{C}_{27}\text{H}_{42}\text{S}^{34}\text{S}^{107}\text{Ag}]^+$	-12
539.17368	6.4	$[\text{C}_{30}\text{H}_{38}\text{S}^{109}\text{Ag}]^+$	99
539.17698	70.8	$[\text{C}_{27}\text{H}_{42}\text{S}_2^{109}\text{Ag}]^+$	-33
539.18960	13.9	$[\text{C}_{30}\text{H}_{40}\text{S}^{107}\text{Ag}]^+$	-23
539.19297	34.5	$[\text{C}_{27}\text{H}_{44}\text{S}_2^{107}\text{Ag}]^+$	-24
539.24711	5.2	$[\text{C}_{28}\text{H}_{48}\text{OS}^{107}\text{Ag}]^+$	-32
539.26751	31.8	$[\text{C}_{29}\text{H}_{50}\text{S}^{109}\text{Ag}]^+$	-31
539.28350	24.5	$[\text{C}_{29}\text{H}_{52}\text{S}^{107}\text{Ag}]^+$	-23

(+) ESI 9.4 T FT-ICR MS of Canadian Bitumen HVGO (475–500°C) with AgOTf

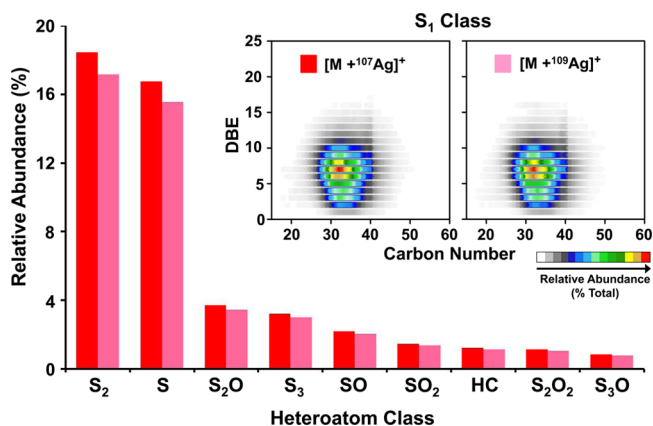


**Figure 2.** Heteroatom class distributions for Canadian bitumen HVGO (475–500 °C) derived from (+) ESI with AgOTf. The abundances of  $[\text{M} + ^{107}\text{Ag}]^+$  and  $[\text{M} + ^{109}\text{Ag}]^+$  ions for each class corresponds to the natural isotopic natural abundances of  $^{107}\text{Ag}$  and  $^{109}\text{Ag}$ . (Inset) Isoabundance-contoured DBE versus carbon number plots for members of the  $\text{S}_1$  class derived from cationization by  $^{107}\text{Ag}^+$  or  $^{109}\text{Ag}^+$ .

over non-basic classes that cannot form  $[\text{M} + \text{H}]^+$  ions. In contrast, cationization with  $\text{Ag}^+$  ionizes non-basic class components ( $\text{S}_9$ ,  $\text{S}_9\text{O}_9$ , and HC). In fact,  $\text{S}_1$  and  $\text{S}_2$  classes are

(+) ESI 9.4 FT-ICR MS with AgOTf ( $[M+Ag]^+$  ions) or HCOOH ( $[M+H]^+$  ions)

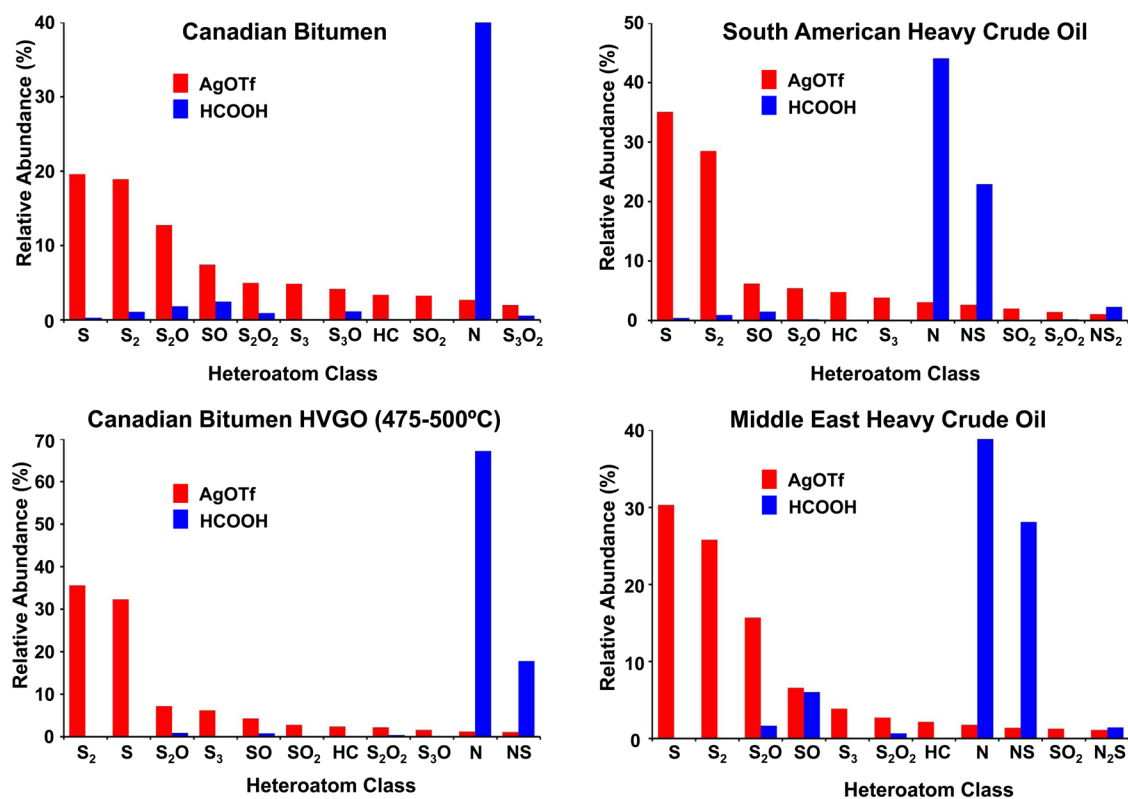


**Figure 3.** Heteroatom class distributions derived from silver cationization ( $[M + ^{107}Ag]^+$  ions) versus conventional formic acid ( $[M + H]^+$  ions) ESI for Canadian bitumen, Canadian bitumen HVGO, a South American heavy crude oil, and a Middle East heavy crude oil.

the most abundant with silver cationization, whereas they are not detected at all by conventional ESI.

With silver cationization, the relative abundances of  $S_1$  and  $S_2$  classes are dramatically higher and a sulfur atom is much more nucleophilic than an oxygen or nitrogen atom and is a softer Lewis base. Sulfur-containing compounds thus preferentially form  $[M + Ag]^+$  adducts. Moreover, the relative abundances of  $S_xO_y$  classes ( $S_1O_1$ ,  $S_1O_2$ ,  $S_2O_1$ ,  $S_2O_2$ ,  $S_3O_1$ , etc.) are also notably higher with silver complexation than conventional ESI. Finally, the interaction of  $Ag^+$  ion with the  $\pi$  electrons of an aromatic ring results in cationization of (nonpolar) HC class species that are absent in conventional positive-ion ESI mass spectra.

**$S_1$ ,  $S_2$ , and  $S_3$  Classes.** Figure 4 contains isoabundance-contoured DBE versus carbon number plots for members of the  $S_1$ ,  $S_2$ , and  $S_3$  classes from the four petroleum samples. The  $S_1$  class for Canadian bitumen extends from DBE  $\sim 2$  to 15 with a carbon number distribution from  $\sim 18$  to 42. As expected, Canadian bitumen HVGO (475–500 °C) exhibits a narrower distribution than its parent bitumen for all heteroatom classes and effectively reveals the Boduszynski progression with an increasing sulfur content from  $S_1$  to  $S_3$ ; for example, its  $S_1$  class ranges from DBE  $\sim 2$  to 11 and carbon number from  $\sim 26$  to 40, centered at  $C_{32}$ , and the  $S_2$  and  $S_3$  classes shift downward in carbon number ( $\sim 3$  carbons per addition of sulfur) because of the increased boiling point associated with an increase in the sulfur number. South American and Middle East crude oils have similar  $S_1$  class distributions, with DBE ranging from  $\sim 1$  to 10 and carbon number from  $\sim 15$  to 35. The maximum DBE versus carbon number abundance for the crude oils lies at carbon number of  $\sim 20$  and DBE of  $\sim 1$  for Middle East crude

and DBE of  $\sim 2$  for South American oil. Such low DBE values for the  $S_1$  class apparently correspond to cyclic sulfides in those samples.

The  $S_2$  class for Canadian bitumen and South American and Middle East crude oils spans an even wider range of DBE and carbon number: bitumen, DBE of  $\sim 2$ –16 and carbon number of  $\sim 20$ –55; South American crude, DBE of  $\sim 2$ –13 and carbon number of  $\sim 10$ –53; and Middle East crude oil, DBE of  $\sim 2$ –15 and carbon number of  $\sim 20$ –68.  $S_3$  class ions are relatively less abundant in the mass spectra of all four samples but still span wide DBE and carbon number ranges for bitumen and the crude oils. The maximum abundances for each of those three samples shift to higher DBE and carbon number values with an increasing number of sulfur atoms. In contrast,  $S_1$ ,  $S_2$ , and  $S_3$  classes from Canadian bitumen HVGO span approximately the same DBE and carbon number range. Behavior of compounds that boil in the same high-temperature range (475–500 °C) but have different numbers of sulfur atoms suggests an absence of intermolecular hydrogen bonding, with sulfur in the form of sulfides, disulfides, and thiophenes rather than thiols.

**$S_xO_y$  Classes.** Figure 5 shows isoabundance-contoured plots of DBE versus carbon number for  $S_1O_1$ ,  $S_2O_1$ , and  $S_3O_1$  classes, derived from Canadian bitumen with silver or HCOOH cationization. Cationization with silver triflate efficiently ionizes those  $S_xO_y$  classes over a wider DBE and carbon number range.  $S_1O_1$  class members from the (+) ESI FT-ICR mass spectrum of bitumen with AgOTf span a DBE range of  $\sim 1$ –14 and carbon number range of  $\sim 10$ –47 compared to a narrower range of DBE ( $\sim 2$ –11) and carbon number ( $\sim 12$ –45) for conventional (+) ESI with formic acid. A similar behavior ( $Ag^+$  cationization versus protonation) is observed for the other  $S_xO_y$

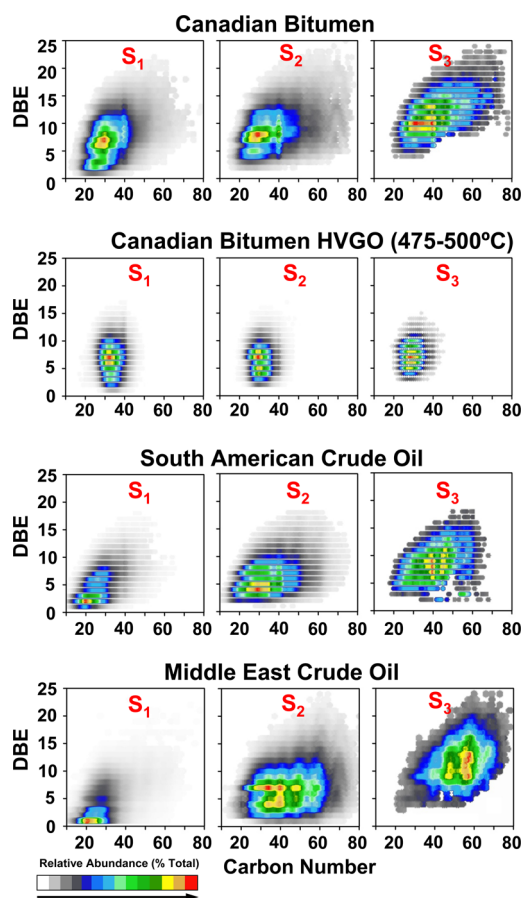


**Figure 4.** Isoabundance-contoured DBE versus carbon number plots for  $S_1$ ,  $S_2$ , and  $S_3$  classes for Canadian bitumen, Canadian bitumen HVGO (475–500 °C), a South American heavy crude oil, and a Middle East heavy crude oil. Silver cationization enables rapid speciation of sulfur species.

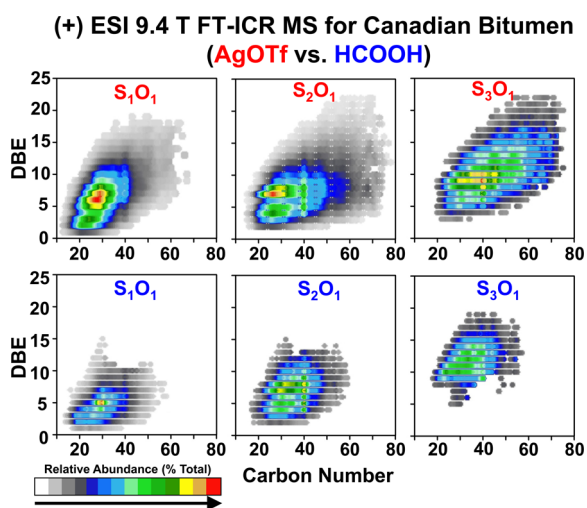


**Figure 5.** Isoabundance-contoured DBE versus carbon number plots for the  $S_1O_1$ ,  $S_2O_1$ , and  $S_3O_1$  classes from Canadian bitumen with AgOTf (top) and HCOOH (bottom).

classes: Ag<sup>+</sup> cationization achieves speciation over a DBE and carbon number range of  $\sim 2$ –14 and  $\sim 17$ –61 for the  $S_2O_1$  class and  $\sim 4$ –23 and  $\sim 20$ –74 for the  $S_3O_1$  class compared to a DBE and carbon number range of  $\sim 2$ –14 and  $\sim 20$ –5 for the  $O_1S_2$  class and a DBE and carbon number range of  $\sim 5$ –19 and

$\sim 20$ –56 for the  $O_1S_3$  class. Note that the increase in the number of heteroatoms in the  $S_nO_m$  classes ( $S_1O_1 < S_2O_1 < S_3O_1$ ) increases the DBE and carbon number values, especially for silver cationization.

**HC Class.** Finally, Figure 6 shows DBE versus carbon number plots for the HC class ions from Canadian bitumen,

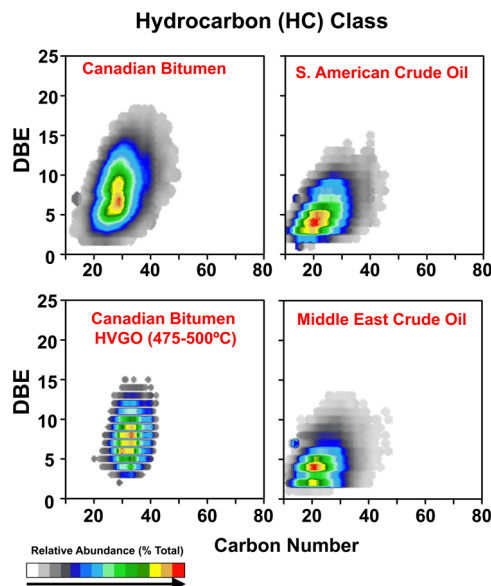


**Figure 6.** Isoabundance-contoured DBE versus carbon number plots for the HC class, derived from silver cationization, followed by positive-ion ESI FT-ICR MS for Canadian bitumen, Canadian bitumen HVGO, a South American heavy crude oil, and a Middle East heavy crude oil.

Canadian bitumen HVGO, and South American and Middle East crude oils. HC class ions from Canadian bitumen exhibit DBE values of 3–16 and carbon numbers of 19–43 with the highest abundance DBE of 7 and the highest abundance carbon number of  $\sim 28$ , consistent with alkylnaphthalenes. As for the  $S_3$  classes, Canadian bitumen distillate exhibits narrower distributions in HC class DBE ( $\sim 3$ –13) and carbon number ( $\sim 23$ –41) than its parent bitumen. South American and Middle East crude oils have similar HC DBE ( $\sim 2$ –10, with a maximum of 4) and carbon number ( $\sim 11$ –33, with a maximum of  $\sim 20$ ) distributions.

It is interesting to note that silver cationization enables the detection of (non-aromatic) HCs with DBE < 4. Those compounds ( $1 \leq \text{DBE} < 4$ ) may correspond to cycloalkanes for crude oil samples and perhaps olefins/cycloalkanes for Canadian bitumen HVGO. The formation of silver adducts based on the use of other silver salts has previously been reported for paraffins, cycloparaffins, and olefins based on matrix-assisted laser desorption ionization (MALDI) and laser desorption ionization (LDI)<sup>54–56</sup> and has even been used for quantitative characterization of a crude oil<sup>57</sup> and petroleum-derived products.<sup>58</sup>

We also allowed silver triflate to react with the oil sample solutions overnight to find out if extending the reaction period would enhance the ionization efficiency. However, overnight stirring yielded essentially the same results as rapid mixing. In contrast, the S-methylation reaction requires 48 h of stirring, followed by processing, whereas cationization with the silver triflate method takes only about 1 min before spraying. Silver triflate has excellent solubility in petroleum solvents and can be

used in the same solvents employed in conventional ESI of crude oils (namely, toluene and methanol).

## AUTHOR INFORMATION

### Corresponding Authors

\*Telephone: +1-850-644-2398. Fax: +1-850-644-1366. E-mail: roddgers@magnet.fsu.edu.

\*Telephone: +1-850-644-0529. Fax: +1-850-644-1366. E-mail: marshall@magnet.fsu.edu.

### Notes

The authors declare no competing financial interest.

## ACKNOWLEDGMENTS

The authors thank Dr. Parviz Rahimi (CanmetENERGY, Devon, Alberta, Canada) for the bitumen samples. This work was supported by the National Science Foundation (DMR-11-57490), the Florida State University Future Fuels Institute, and the State of Florida.

## REFERENCES

- (1) Wang, D.; Qian, E. W.; Amano, H.; Okata, K.; Ishihara, A.; Kabe, T. *Appl. Catal., A* **2003**, *253*, 91–99.
- (2) Babich, I. V.; Moulijn, J. A. *Fuel* **2003**, *82*, 607–631.
- (3) Song, C. *Catal. Today* **2003**, *86*, 211–263.
- (4) Yang, R. T.; Hernandez-Maldonado, A. J.; Yang, F. H. *Science* **2003**, *301*, 79–81.
- (5) Choudhary, T. V. *Ind. Eng. Chem. Res.* **2007**, *46*, 8363–8370.
- (6) Gates, B. C.; Topsoe, H. *Polyhedron* **1997**, *16*, 3213–3217.
- (7) Breyse, M.; Djega-Mariadassou, G.; Pessayre, S.; Geantet, C.; Vrinat, M.; Perot, G.; Lemaire, M. *Catal. Today* **2003**, *84*, 129–138.
- (8) Aragon, P. E.; Romero, J.; Negrete, P.; Sharma, V. K. *J. Environ. Sci. Health, Part A: Toxic/Hazard. Subst. Environ. Eng.* **2005**, *40*, 553–558.
- (9) Gupta, N.; Roychoudhury, P. K.; Deb, J. K. *Appl. Microbiol. Biotechnol.* **2005**, *66*, 356–366.
- (10) Shiraishi, Y.; Hirai, T. *Energy Fuels* **2004**, *18*, 37–40.
- (11) Marshall, A. G.; Hendrickson, C. L.; Jackson, G. S. *Mass Spectrom. Rev.* **1998**, *17*, 1–35.
- (12) Hughey, C. A.; Hendrickson, C. L.; Rodgers, R. P.; Marshall, A. G.; Qian, K. *Anal. Chem.* **2001**, *73*, 4676–4681.
- (13) Hughey, C. A.; Rodgers, R. P.; Marshall, A. G. *Anal. Chem.* **2002**, *74*, 4145–4149.
- (14) Kim, S.; Stanford, L. A.; Rodgers, R. P.; Marshall, A. G.; Walters, C. C.; Qian, K.; Wenger, L. M.; Mankiewicz, P. *Org. Geochem.* **2005**, *36*, 1117–1134.
- (15) Klein, G. C.; Kim, S.; Rodgers, R. P.; Marshall, A. G.; Yen, A.; Asomaning, S. *Energy Fuels* **2006**, *20*, 1965–1972.
- (16) Klein, G. C.; Rodgers, R. P.; Marshall, A. G. *Fuel* **2006**, *85*, 2071–2080.
- (17) Marshall, A. G.; Rodgers, R. P. *Acc. Chem. Res.* **2004**, *37*, 53–59.
- (18) Purcell, J. M.; Hendrickson, C. L.; Rodgers, R. P.; Marshall, A. G. *Anal. Chem.* **2006**, *78*, 5906–5912.
- (19) Purcell, J. M.; Hendrickson, C. L.; Rodgers, R. P.; Marshall, A. G. *J. Am. Soc. Mass Spectrom.* **2007**, *18*, 1682–1689.
- (20) Purcell, J. M.; Juyal, P.; Kim, D.-G.; Rodgers, R. P.; Hendrickson, C. L.; Marshall, A. G. *Energy Fuels* **2007**, *21*, 2869–2874.
- (21) Purcell, J. M.; Rodgers, R. P.; Hendrickson, C. L.; Marshall, A. G. *J. Am. Soc. Mass Spectrom.* **2007**, *18*, 1265–1273.
- (22) Qian, K.; Robbins, W. K.; Hughey, C. A.; Cooper, H. J.; Rodgers, R. P.; Marshall, A. G. *Energy Fuels* **2001**, *15*, 1505–1511.
- (23) Qian, K.; Rodgers, R. P.; Hendrickson, C. L.; Emmett, M. R.; Marshall, A. G. *Energy Fuels* **2001**, *15*, 492–498.
- (24) Rodgers, R. P.; Marshall, A. G. In *Asphaltenes, Heavy Oils, and Petroleomics*; Mullins, O. C., Sheu, E. Y., Hammani, A., Marshall, A. G., Eds.; Springer: New York, 2007; pp 63–89.
- (25) Rodgers, R. P.; Schaub, T. M.; Marshall, A. G. *Anal. Chem.* **2005**, *77*, 20A–27A.
- (26) Schaub, T. M.; Rodgers, R. P.; Marshall, A. G.; Qian, K.; Green, L. A.; Olmstead, W. N. *Energy Fuels* **2005**, *19*, 1566–1573.
- (27) Smith, D. F.; Schaub, T. M.; Kim, S.; Rodgers, R. P.; Rahimi, P.; Teclemariam, A.; Marshall, A. G. *Energy Fuels* **2008**, *22*, 2372–2378.
- (28) Smith, D. F.; Schaub, T. M.; Rahimi, P.; Teclemariam, A.; Rodgers, R. P.; Marshall, A. G. *Energy Fuels* **2007**, *21*, 1309–1316.
- (29) Fenn, J. B.; Mann, M.; Meng, C. K.; Wong, S. F.; Whitehouse, C. M. *Science* **1989**, *246*, 64–71.
- (30) Fenn, J. B.; Mann, M.; Meng, C. K.; Wong, S. F.; Whitehouse, C. M. *Mass Spectrom. Rev.* **1990**, *9*, 37–70.
- (31) Wilkinson, G. *Comprehensive Coordination Chemistry: The Synthesis, Reactions, Properties and Applications of Coordination Compounds*; Pergamon Press: Oxford, U.K., 1987.
- (32) Headley, J. V.; Peru, K. M.; Armstrong, S. A.; Han, X. M.; Martin, J. W.; Mapolelo, M. M.; Smith, D. F.; Rogers, R. P.; Marshall, A. G. *Rapid Commun. Mass Spectrom.* **2009**, *23*, 515–522.
- (33) Headley, J. V.; Peru, K. M.; Mishra, S.; Meda, V.; Dalai, A. K.; McMartin, D. W.; Mapolelo, M. M.; Rodgers, R. P.; Marshall, A. G. *Rapid Commun. Mass Spectrom.* **2010**, *24*, 3121–3126.
- (34) Hughey, C. A.; Minardi, C. S.; Galasso-Roth, S. A.; Paspalof, G. B.; Mapolelo, M. M.; Rodgers, R. P.; Marshall, A. G.; Ruderman, D. L. *Rapid Commun. Mass Spectrom.* **2008**, *22*, 3968–3976.
- (35) Mapolelo, M. M.; Rodgers, R. P.; Blakney, G. T.; Yen, A. T.; Asomaning, S.; Marshall, A. G. *Int. J. Mass Spectrom.* **2011**, *300*, 149–157.
- (36) Mapolelo, M. M.; Stanford, L. A.; Rodgers, R. P.; Yen, A. T.; Debord, J. D.; Asomaning, S.; Marshall, A. G. *Energy Fuels* **2009**, *23*, 349–355.
- (37) Quirke, J. M. E.; Adams, C. L.; Van Berkel, G. J. *Anal. Chem.* **1994**, *66*, 1302–1315.
- (38) Van Berkel, G. J.; Asano, K. G. *Anal. Chem.* **1994**, *66*, 2096–2102.
- (39) Mueller, H.; Andersson, J. T.; Schrader, W. *Anal. Chem.* **2005**, *77*, 2536–2543.
- (40) Roussis, S. G.; Proulx, R. *Anal. Chem.* **2002**, *74*, 1408–1414.
- (41) Roussis, S. G.; Proulx, R. *Rapid Commun. Mass Spectrom.* **2004**, *18*, 1761–1775.
- (42) Canty, A. J.; Colton, R. *Inorg. Chim. Acta* **1994**, *220*, 99–105.
- (43) Gruendling, T.; Hart-Smith, G.; Davis, T. P.; Stenzel, M. H.; Barner-Kowollik, C. *Macromolecules* **2008**, *41*, 1966–1971.
- (44) Laali, K. K.; Hupertz, S.; Temu, A. G.; Galembeck, S. E. *Org. Biomol. Chem.* **2005**, *3*, 2319–2326.
- (45) Rudzinski, W. E.; Zhou, K.; Luo, X. *Energy Fuels* **2004**, *18*, 16–21.
- (46) Senko, M. W.; Hendrickson, C. L.; Pasa-Tolic, L.; Marto, J. A.; White, F. M.; Guan, S.; Marshall, A. G. *Rapid Commun. Mass Spectrom.* **1996**, *10*, 1824–1828.
- (47) Blakney, G. T.; Hendrickson, C. L.; Marshall, A. G. *Int. J. Mass Spectrom.* **2011**, *306*, 246–252.
- (48) Emmett, M. R.; White, F. M.; Hendrickson, C. L.; Shi, S. D. H.; Marshall, A. G. *J. Am. Soc. Mass Spectrom.* **1998**, *9*, 333–340.
- (49) Senko, M. W.; Hendrickson, C. L.; Emmett, M. R.; Shi, S. D. H.; Marshall, A. G. *J. Am. Soc. Mass Spectrom.* **1997**, *8*, 970–976.
- (50) Wilcox, B. E.; Hendrickson, C. L.; Marshall, A. G. *J. Am. Soc. Mass Spectrom.* **2002**, *13*, 1304–1312.
- (51) Kendrick, E. *Anal. Chem.* **1963**, *35*, 2146–2154.
- (52) McLafferty, F. W.; Tureek, F. *Interpretation of Mass Spectra*, 4th ed.; University Science Books: Sausalito, CA, 1993; p 371.
- (53) Inoue, Y.; Gokel, G. W. *Cation Binding by Macrocycles*; Marcel Dekker, Inc.: New York, 1990.
- (54) Chen, R.; Li, L. *J. Am. Soc. Mass Spectrom.* **2001**, *12*, 367–375.
- (55) Pruns, J. K.; Vietzke, J. P.; Strassner, M.; Rapp, C.; Hintze, U.; Konig, W. A. *Rapid Commun. Mass Spectrom.* **2002**, *16*, 208–211.
- (56) Sherrod, S. D.; Diaz, A. J.; Russell, W. K.; Cremer, P. S.; Russell, D. H. *Anal. Chem.* **2008**, *80*, 6796–6799.
- (57) Dutta, T. K.; Harayama, S. *Anal. Chem.* **2001**, *73*, 864–869.
- (58) Pruns, J. K.; Rapp, C.; Hintze, U.; Wittner, K. P.; Konig, W. A. *Eur. J. Lipid Sci. Technol.* **2003**, *105*, 275–280.